

ANNz: estimating photometric redshifts using artificial neural networks

Adrian A. Collister¹*, Ofer Lahav¹

¹ Institute of Astronomy, University of Cambridge, Cambridge, CB3 0HA, UK

ABSTRACT

We introduce ANNz, a freely available software package for photometric redshift estimation using Artificial Neural Networks. ANNz learns the relation between photometry and redshift from an appropriate training set of galaxies for which the redshift is already known. Where a large and representative training set is available ANNz is a highly competitive tool when compared with traditional template-fitting methods.

The ANNz package is demonstrated on the Sloan Digital Sky Survey Data Release 1. The r.m.s. redshift error in the range $0 \lesssim z \lesssim 0.7$ is $\sigma_{\text{rms}} = 0.024$. Various extensions to the basic method are demonstrated using the Sloan Data. Finally, more realistic conditions (spectroscopic sets which are small, or which are brighter than the photometric set for which redshifts are required) are simulated and the impact on the photometric redshift accuracy assessed.

The package may be freely downloaded from <http://www.ast.cam.ac.uk/~aac>.

Key words: surveys – galaxies: distances and redshifts – methods: data analysis

1 INTRODUCTION

In its most general sense, the term *photometric redshift* refers to a redshift estimated using only medium- or broad-band photometry or imaging. Most commonly, photometric redshifts are determined on the basis of galaxies’ colours in three or more filters (thus giving a very coarse approximation to the spectral energy distribution, hereafter SED), but they could also be based on other properties which can be derived from images, such as the angular size or concentration index. The method has found successful application to deep-field and wide-field surveys, notably the Hubble Deep Field (e.g. Fernández-Soto, Lanzetta & Yahil 1999), and the Sloan Digital Sky Survey (Csabai et al. 2003).

The most commonly used approach to photometric redshift estimation is the *template-matching* technique. This requires a set of ‘template’ SEDs covering a range of galaxy types, luminosities and redshifts appropriate to the population for which photometric redshifts are required. For a particular target galaxy, the photometric redshift is chosen to be the redshift of the most closely matching template spectrum; this is usually defined as the template which minimizes the χ^2 between the template and actual magnitudes.

The template spectra are usually derived from a small set of SEDs representing different classes of galaxy at redshift $z = 0$, which are then manually redshifted to give a

discrete sampling along the redshift axis (note then, that this method allows for no *evolution* with redshift). Commonly used template sets are the Coleman, Wu & Weedman (CWW; 1980) SEDs which are derived observationally, or those of Bruzual & Charlot (1993), derived from population synthesis models. The template-matching technique owes its popularity to the very few resources required for a basic implementation (i.e. a handful of template SEDs), but the accuracy of the technique strongly depends on the extent to which the template spectra are representative of the target populations: for example, template SEDs derived from observations of low-redshift galaxy populations may be a poor match for populations at higher redshifts.

The chances of success can be improved by increasing the number of templates, or by more carefully matching the templates to the populations being studied. For example, the spectroscopic catalogue of the Sloan Digital Sky Survey (SDSS; York et al. 2000) could be used to produce a set of templates which are very well representative of the SDSS photometric catalogue (Csabai et al. 2003). However, in situations with such a large amount of prior redshift information about the sample, the template-matching technique is not the best approach: so-called *empirical* methods usually offer greater accuracy, as well as being far more efficient.

In essence, empirical photometric redshift methods aim to derive a parametrization for the redshift (as a function of the photometric parameters) from a suitably large and representative *training set* of galaxies (for which we have both photometry and a precisely known redshift). A simple exam-

* aac@ast.cam.ac.uk

ple is to express the redshift as a polynomial in the galaxy colours (e.g. Connolly et al. 1995; Sowards-Emmerd et al. 2000). The coefficients in the polynomial are varied to optimize the fit between the predicted and measured redshift. The photometric redshift for the galaxies for which we have no spectroscopy can then be estimated by applying the optimized function to the colours of the target galaxy.

For a sufficiently sophisticated parametrization, the empirical approach is limited by the quality of the training data. Ideally the training set would be a representative subset of the actual photometric target sample (this has the attractive side-effect of nullifying any systematics in the photometry). In principle however, the training set could also be derived from a set of template spectra or from simulated catalogues (e.g. from semi-analytic models). The photometry for the training set must be for the same filter set and have the same noise characteristics as that for the target sample. The trained method can usually only be reliably applied to target galaxies within the ranges of redshift and spectral type adequately sampled by the training set.

In this paper we introduce ANNz, a software package for photometric redshift estimation using Artificial Neural Networks (hereafter ANNs) to parametrize the redshift-photometry relation. It can be shown (e.g. Jones 1990; Blum & Li 1991) that a sufficiently complex ANN is capable of approximating to arbitrary accuracy any functional continuous mapping. ANNs have previously found a number of applications in astronomy, including morphological classification of galaxies (e.g. Lahav et al. 1996; Ball et al. 2003) and star/galaxy separation (e.g. Andreon et al. 2000). Firth, Lahav & Somerville (2003) previously demonstrated the feasibility of using ANNs for photometric redshift estimation.

The layout of this paper is as follows. In §2 Artificial Neural Networks are introduced, and the particular methods used by ANNz are explained. In §3 ANNz is applied to the Sloan Digital Sky Survey. The results are compared with rival photometric redshift estimators and various extensions to the basic technique are explained and illustrated. Finally, less ideal conditions are simulated to assess the impact on the accuracy of photometric redshift estimation. In §4 the results are summarised, and prospects for the application of ANNz discussed.

2 ARTIFICIAL NEURAL NETWORKS

ANNz uses a particular species of ANN known formally as a *multi-layer perceptron* (MLP). A MLP consists of a number of layers of *nodes* (Fig. 1; see e.g. Bishop 1995, and references therein, for background). The first layer contains the inputs, which in our application to photometric redshift estimation are the magnitudes, m_i , of a galaxy in a number of filters (for ease of notation we arrange these in a vector $\mathbf{m} \equiv (m_1, m_2, \dots, m_n)$). The final layer contains the outputs; we will usually use just one output, the photometric redshift z_{phot} , but see §3.2.2 for an example with multiple outputs. Intervening layers are described as *hidden* and there is complete freedom over the number and size of hidden layers used. The nodes in a given layer are connected to all the nodes in adjacent layers. A particular network architecture may be denoted by $N_{\text{in}}:N_1:N_2:\dots:N_{\text{out}}$ where N_{in} is the

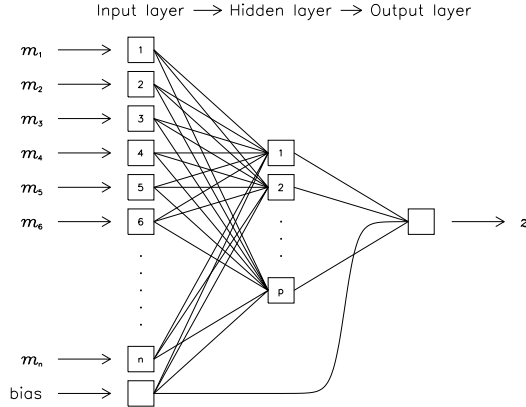


Figure 1. A schematic diagram of a multi-layer perceptron, as implemented by ANNz, with input nodes taking, for example, magnitudes $m_i = -2.5 \log_{10} f_i$ in various filters, a single hidden layer, and a single output node giving, for example, redshift z . The architecture is $n:p:1$ in the notation used in this paper. Each connecting line carries a weight w_{ij} . The bias node allows for an additive constant in the network function defined at each node. More complex networks can have additional hidden layers and/or outputs.

number of input nodes, N_1 is the number of nodes in the first hidden layer, and so on. For example 9:6:1 takes 9 inputs, has 6 nodes in a single hidden layer and gives a single output.

Each connection carries a weight, w_{ij} ; these comprise the vector of coefficients, \mathbf{w} , which are to be optimized. An *activation function*, $g_j(u_j)$, is defined at each node, taking as its argument

$$u_j = \sum_i w_{ij} g_i(u_i), \quad (1)$$

where the sum is over all nodes i sending connections to node j . The activation functions are typically taken (in analogy to biological neurons) to be sigmoid functions such as $g_j(u_j) = 1/[1 + \exp(-u_j)]$, and we follow this approach here. An extra input node – the bias node – is automatically included to allow for additive constants in these functions.

For a particular input vector, the output vector of the network is determined by progressing sequentially through the network layers, from inputs to outputs, calculating the activation of each node (hence this type of neural network is often referred to as a *feed-forward* network).

Given a suitable training set of galaxies for which we have both photometry, \mathbf{m} , and a spectroscopic redshift, z_{spec} , the ANN is trained by minimizing the *cost function*

$$E = \sum_k (z_{\text{phot},k}(\mathbf{w}, \mathbf{m}_k) - z_{\text{spec},k})^2, \quad (2)$$

with respect to the weights, \mathbf{w} , where $z_{\text{phot},k}(\mathbf{w}, \mathbf{m}_k)$ is the network output for the given input and weight vectors, and the sum is over the galaxies in the training set. To ensure that the weights are regularized (i.e. that they do not become too large), an extra quadratic cost term

$$E_w = \beta \sum_{i,j} w_{ij}^2, \quad (3)$$

is added to equation 2.

ANNz uses an iterative quasi-Newton method to perform this minimization. Details of the minimization algorithm and regularization may be found in Bishop (1995) and Lahav et al. (1996, Appendices).

After each training iteration, the cost function is also evaluated on a separate *validation* set. After a chosen number of training iterations, training terminates and the final weights chosen for the ANN are those from the iteration at which the cost function is minimal on the *validation* set. This is useful to avoid over-fitting to the training set if the training set is small. The trained network may then be presented with previously unseen input vectors, and the outputs computed.

2.1 Photometric noise

In real situations the inputs to the network (e.g. the magnitudes in this case of photometric redshift estimation) will usually have a measurement noise associated with them. We can assess the variance these errors effect in the output using the usual chain-rule approach:

$$\sigma_z^2 = \sum_i \left(\frac{\partial z}{\partial m_i} \right)^2 \sigma_{m_i}^2, \quad (4)$$

where the sum is over the network inputs.

Given a trained network, the output is an analytic function of the network weights and the input vector: $z = z(\mathbf{w}, \mathbf{m})$. Provided the activation functions, $g_i(u_i)$, are differentiable, the derivatives $\partial z / \partial m_i$ can be obtained through a simple and efficient algorithm (Bishop 1995, pp.148–150). This method is used by *ANNz* to estimate the variance in its photometric redshifts due to the photometric noise.

2.2 Network variance

Prior to training, *ANNz* randomizes the initial values of the weights. Depending on the particular initialization state used, the training process will usually converge to different local minima of the cost function. A common practice is to train a number of networks and select one based on the best performance on the validation set. However, this is wasteful of training effort and, in fact, the sub-optimal networks can be used to improve overall accuracy: the mean of the individual outputs of a group of networks (known as a *committee*) will usually be a more accurate estimate for the true redshift than the outputs of any one committee member in isolation.

Using a committee also allows the uncertainty in the output due to the variance in the network weights to be estimated. For a particular target galaxy the photometric redshift prediction should ideally be robust to different initializations of the weight vector. However, it may be the case that the available photometry or training set does not constrain the redshift very well (even for high signal-to-noise photometry, so the error estimated by the method of §2.1 could be relatively small). These cases are more likely to show a large variance in the output for different initializations of the weight vector, hence using a committee may assist in their identification. *ANNz* allows arbitrarily large committees to be used, and estimates the contribution of

the network variance to the error in the photometric redshift for each galaxy in the testing set.

2.3 The *ANNz* package

ANNz comprises two main programs, `annz_train` and `annz_test`. The first takes as its inputs a network architecture together with training and validation data sets. It trains the network on the given data, as described above, and saves the final weights vector to file.

The second program submits a test data set to one or more trained networks. If the program is provided with more than two trained networks, it automatically applies the committee methods of §2.2.

We have made *ANNz* available on the WWW at the following address: <http://www.ast.cam.ac.uk/~aac>. Full instructions are provided with the package.

3 APPLICATION TO SDSS DATA

In their First Data Release (DR1), the Sloan Digital Sky Survey¹ (SDSS; York et al. 2000) consortium released spectroscopic redshifts along with *ugriz* photometry and various image morphological parameters for over 130,000 galaxies. These provide an excellent opportunity to test the performance of *ANNz* on real data.

The selection algorithm for the SDSS spectroscopic survey results in two subsets of the data: a main galaxy catalogue and a luminous red galaxy catalogue (LRG; Eisenstein et al. 2001). The main galaxy catalogue is a flux-limited sample ($r < 17.77$) with a median redshift $z = 0.104$ (Strauss et al. 2002), while the LRG catalogue is flux- and colour-selected to be a very uniform and approximately volume-limited sample (it is volume limited to $z \approx 0.4$, but probes out to $z \approx 0.6$ at lower completion).

3.1 Comparison with other techniques

The SDSS consortium have themselves applied a range of photometric redshift techniques to their commissioning data (Csabai et al. 2003). Table 1 lists the estimation errors they obtained. This commissioning data was made public in the Early Data Release (EDR; Stoughton et al. 2002). In order to allow a direct comparison of the accuracy of *ANNz* with the methods used by Csabai et al. (2003) we selected

¹ Funding for the creation and distribution of the SDSS Archive has been provided by the Alfred P. Sloan Foundation, the Participating Institutions, the National Aeronautics and Space Administration, the National Science Foundation, the U.S. Department of Energy, the Japanese Monbukagakusho, and the Max Planck Society. The SDSS Web site is <http://www.sdss.org/>.

The SDSS is managed by the Astrophysical Research Consortium (ARC) for the Participating Institutions. The Participating Institutions are The University of Chicago, Fermilab, the Institute for Advanced Study, the Japan Participation Group, The Johns Hopkins University, Los Alamos National Laboratory, the Max-Planck-Institute for Astronomy (MPIA), the Max-Planck-Institute for Astrophysics (MPA), New Mexico State University, University of Pittsburgh, Princeton University, the United States Naval Observatory, and the University of Washington.

Table 1. Errors on photometric redshifts obtained by Csabai et al. (2003) for the SDSS Early Data Release. The first five methods use the basic template-matching technique described in §1. The accuracy is progressively improved by increasing the number of template spectra and improving the extent to which they represent the target sample. The nearest-neighbour method is essentially template-matching using the entire EDR spectroscopic catalogue as the template set: the best-fitting template is defined as that being closest to the target galaxy in colour-space. Polynomial and Kd-tree are empirical methods trained on the whole spectroscopic catalogue. The result obtained using ANNz is appended for comparison. $\sigma_{\text{rms}}^2 = \langle (z_{\text{phot}} - z_{\text{spec}})^2 \rangle$.

Estimation method	σ_{rms}
CWW	0.0666
Bruzual-Charlot	0.0552
CWW LRG	0.0473
Repaired LRG	0.0476
Interpolated	0.0451
Nearest-neighbour	0.0365
Polynomial	0.0318
Kd-tree	0.0254
ANNz	0.0238

the main galaxy and LRG samples from the EDR. From these $\sim 30,000$ galaxies we randomly selected training, validation and testing sets with respective sizes 15,000, 5,000 and 10,000. The network inputs were the galaxy magnitudes in each of the five filters and the overall architecture was 5:10:10:1. Figure 2 shows the ANNz photometric redshifts against the spectroscopic values. The rms deviation between these is $\sigma_{\text{rms}} = \sqrt{\langle (z_{\text{phot}} - z_{\text{spec}})^2 \rangle} = 0.0238$, which compares well with the results in Table 1.

HYPERZ (Bolzonella, Miralles & Pelló 2000) is a widely used template-based photometric redshift package. In order to more directly compare ANNz with the template-matching method, **HYPERZ** was applied to the same testing set using the CWW template SEDs (Coleman et al. 1980). It is clear from the results in Fig. 2 that not only is the rms dispersion in the photometric redshift considerably greater than that for ANNz , but there are also significant systematic deviations in the **HYPERZ** results. ANNz also suffers very few catastrophic failures, whereas **HYPERZ** seems to completely misjudge the redshift in many cases. The SDSS consortium obtained similar accuracies using the simplest template-based approach (results labelled *CWW* and *Bruzual-Charlot* in Table 1). With more sophisticated template-based methods they were able to improve on these errors, but still do not match the accuracy achieved by the empirical methods.

3.2 Application to Data Release 1

The rest of this work is based on data from the SDSS DR1. The combined main galaxy and LRG samples in the DR1 spectroscopic catalogue amount to $\sim 125,000$ galaxies. A committee of five 5:10:10:1 networks was trained on 50,000 DR1 galaxies with a validation set of 10,000, and applied to a testing set of 64,175 galaxies. The results are summarized in Figure 4. We note that the rms deviation is similar to that obtained for the EDR, being $\sigma_{\text{rms}} = 0.0236$. For clarity the errorbars for the photometric redshifts are not shown in this figure. The results for a randomly chosen subset of 200

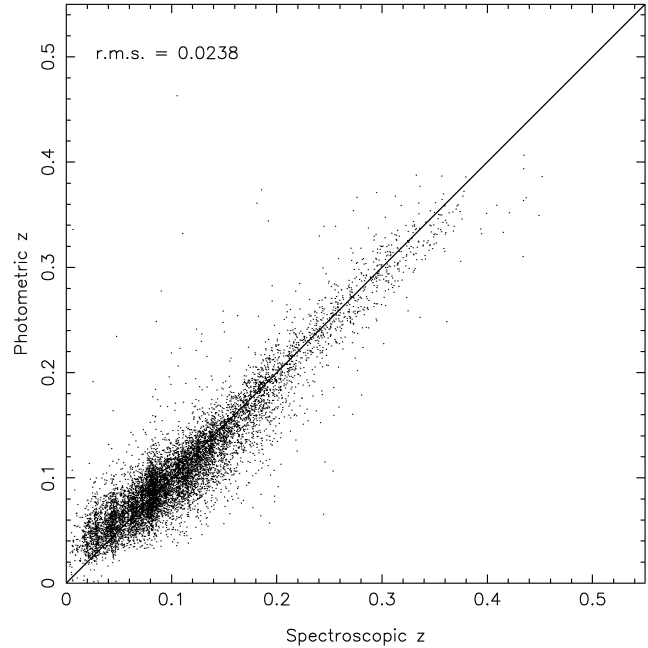


Figure 2. Spectroscopic vs . photometric redshifts for ANNz applied to 10,000 galaxies randomly selected from the SDSS EDR main galaxy and LRG samples. The architecture used was 5:10:10:1.

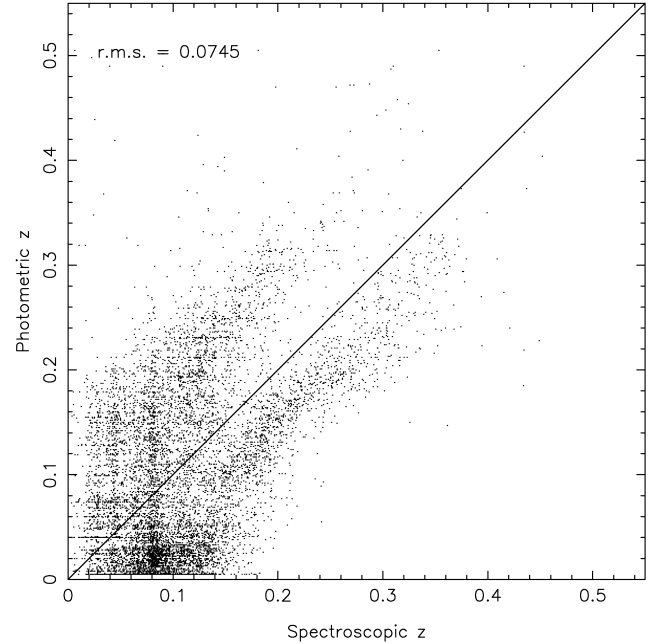


Figure 3. Photometric redshift estimation using **HYPERZ** with the CWW template SEDs. This uses the same 10,000 galaxy sample as figure 2. There are obvious systematic deviations, with bands apparent above and below the $z_{\text{phot}} = z_{\text{spec}}$ line.

galaxies are shown with errorbars in Figure 5. The rms deviations for the individual committee members span a range of $\Delta\sigma_{\text{rms}} = 0.0003$, indicating that the photometric redshift accuracy is very robust to different initializations of the network weights. This is also reflected in the fact that the error bars in this case are dominated by the photometric noise.

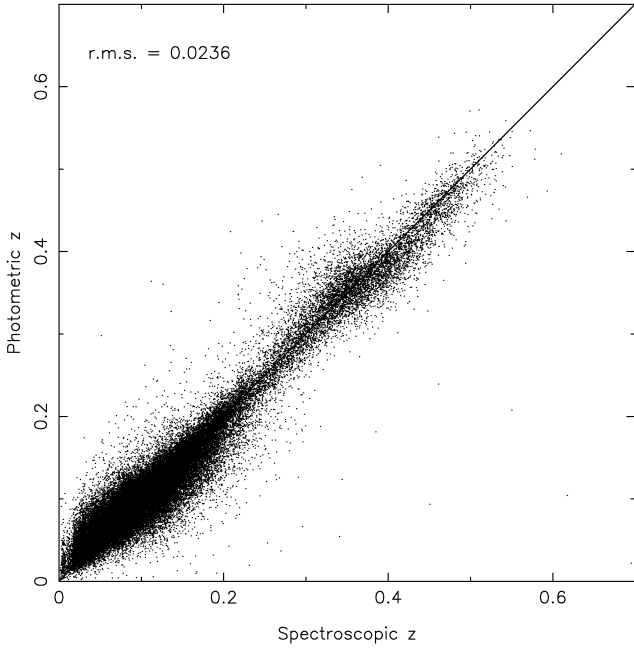


Figure 4. Spectroscopic $vs.$ photometric redshifts for ANNz applied to a testing set of 64,175 galaxies randomly selected from the SDSS DR1 main galaxy and LRG samples. A committee of five 5:10:10:1 networks was used. The apparent bimodality is due to the spectroscopic redshift distributions of the Main and LRG samples.

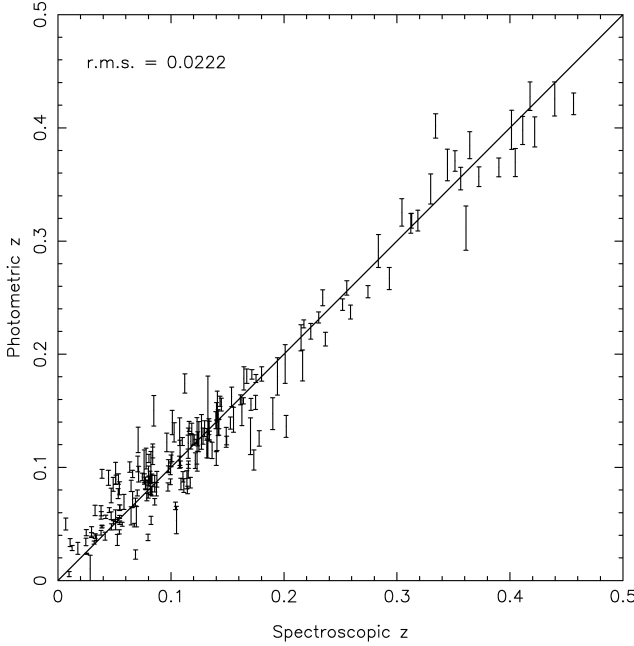


Figure 5. A subset of 200 galaxies randomly selected from the results of Fig. 4, and with the error bars calculated by ANNz shown. These are a combination of contributions from photometric noise (§2.1) and network variance (§2.2).

3.2.1 Using additional inputs

One of the great advantages of empirical photometric redshift methods is the ease with which we can introduce additional observables into our parametrization of the photometric redshift. This is particularly true for ANNz; we simply add an extra input to our network architecture for each new parameter we wish to consider. ANNz treats these new inputs in exactly the same way as it does the galaxy magnitudes.

By way of example, the r -band 50 and 90 per cent Petrosian flux radii were added as two extra inputs to our ANN. These are the angular radii (concentric with the galaxy brightness distribution) containing the stated fraction of the Petrosian flux, and therefore contain information on the angular size of the galaxy (clearly a strongly distance-dependent property) and the *concentration index* (essentially the steepness of the galaxy brightness profile, which may help break degeneracies in the redshift-colour relationship). Running this data set through ANNz (using a committee of five 7:11:11:1 networks) produced a redshift estimation accuracy of $\sigma_{\text{rms}} = 0.0230$, an improvement of ~ 3 per cent compared to the results based only on the magnitudes.

3.2.2 Predicting spectral type

It is equally straightforward to train ANNz to make predictions for properties other than the redshift. Template-matching photometric redshift techniques have the useful side effect of assigning an estimated spectral type to each galaxy, in addition to estimating the redshift. Firth et al. (2003) demonstrated the use of ANNs to determine spectral types from broad-band photometry. The spectroscopic catalogue of the SDSS includes a continuous parameter (`eClass`) indicating spectral type which ranges from approximately -0.5 (early types) to 1 (late types). A 5:10:10:2 network architecture was used to attempt the simultaneous estimation of redshift and `eClass` for the same DR1 galaxies used above. The accuracy of the redshift estimation was not significantly affected, being $\sigma_{\text{rms}} = 0.0241$. The `eClass` was determined with an rms error of $\sigma_{\text{rms}} = 0.0516$ (Fig. 6).

3.3 More realistic conditions

Our example applications to the SDSS in §3.2 are somewhat idealistic, since we are training and testing on samples with identical redshift, magnitude and galaxy species distributions. Furthermore, our training samples have thus far been very large. In this section less optimal training sets are used to investigate their impact on the photometric redshift accuracy.

3.3.1 Smaller training sets

The size of training sample needed will be strongly dependent on the range of redshifts and galaxy types in the target sample. The same testing set of 64,175 galaxies was submitted to networks trained on samples of (i) 2000 galaxies and (ii) 200 galaxies. In both cases the samples were split equally into the training and validation sets. Committees of five 5:10:10:1 networks were used.

The photometric redshift accuracies were respectively

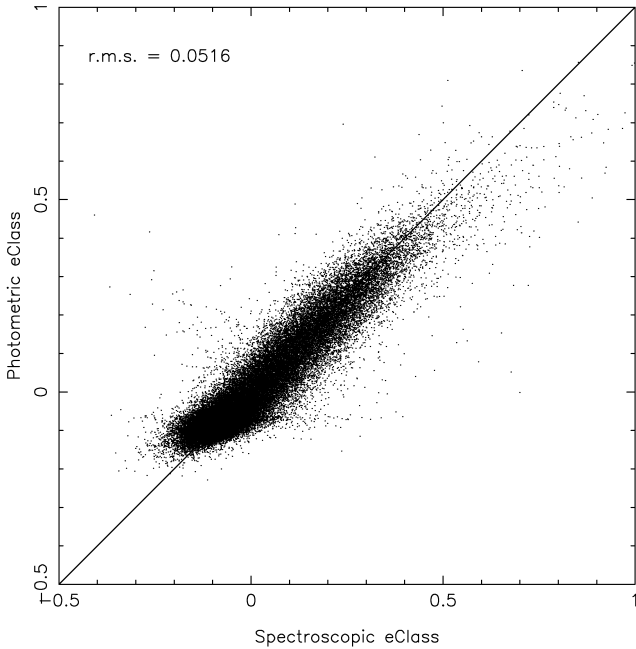


Figure 6. Results from using ANNz to predict the spectral type (in the form of the eClass parameter) simultaneously with the redshift. This is the same testing set of 64,175 galaxies used in Fig. 4.

(i) $\sigma_{\text{rms}} = 0.0263$ and (ii) $\sigma_{\text{rms}} = 0.0343$. In the first case the loss of accuracy is not significant. The second case demonstrates well the problems associated with small training sets. The rarer objects in the sample (e.g. here, those at high redshift) feature very sparsely (if at all) in the training set and so the network is unable to sensibly deal with these objects when they appear in the testing data. This leads to an increased number of outliers and, potentially, the introduction of systematic errors.

3.3.2 Biased training sets

For increasingly faint targets, acquiring good spectroscopy becomes increasingly difficult and eventually prohibitively expensive; this problem is the primary motivation for photometric redshifts. In practice then, the available spectroscopic training sample is likely to be somewhat brighter on average than the photometric target sets. However, the major stumbling block for empirical photometric redshift estimation techniques is the difficulty in applying them outside of the regions of parameter space which are well sampled by the training data: while the estimator ought to be able to interpolate *within* the training regime, extrapolating beyond is much more problematic. Ideally we would like to be able to train our estimator on bright galaxies, and then confidently apply it to faint galaxies.

To assess the effectiveness of ANNz in this situation the Luminous Red Galaxy sample was split roughly in half by imposing a magnitude cut at $r = 18.5$. The brighter sub-sample was further subdivided into training and validation sets of size 5000 and 2000 galaxies respectively. A committee of five 5:10:10:1 networks was trained on this data and then applied to the remaining ~ 6000 LRGs (for which the limiting magnitude is $r \approx 19.6$).

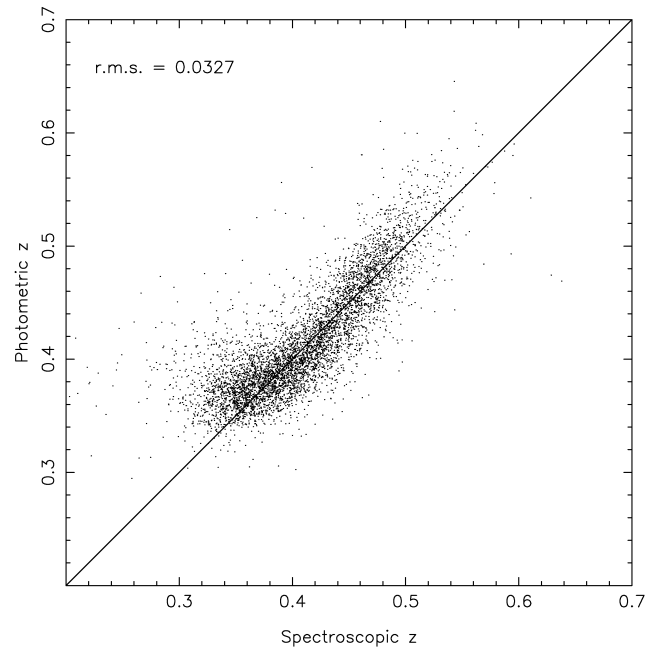


Figure 7. Results from training networks on LRGs with $r < 18.5$, but applied to LRGs with strictly $r > 18.5$ (note the change of intercept of the axes). The limiting magnitude for the LRGs is $r \approx 19.6$.

The results are shown in Fig. 7. The overall dispersion is $\sigma_{\text{rms}} = 0.0327$ which represents only a slight loss of accuracy when compared with results using a LRG training set selected over all magnitudes ($\sigma_{\text{rms}} = 0.0294$). The LRGs are a very uniform sample with respect to spectral types; this may explain why we are able to extrapolate to over a magnitude fainter without significant loss of photometric redshift accuracy.

4 CONCLUSIONS

In appropriate circumstances, ANNz is a highly competitive tool for photometric redshift estimation. However, it does rely on the existence of a sufficiently large training set which is representative of the particular populations being studied. The package's utility therefore lies particularly with large photometric surveys such as the SDSS, GOODS (Dickinson 2001) or the VIRMOS-VLT Deep Survey (Le Fevre et al. 2003), some of which include spectroscopic surveys for subsets of the photometric catalogues (for example, of the eventual 100 million photometric objects which the SDSS expect to catalogue, 1 million will also have spectroscopy, and hence accurate redshifts).

A major problem for empirical photometric redshift estimators is the difficulty in extending the method to regions of colour-space poorly sampled by the training data. Colour-space comparisons are a useful method of matching the training data to the target sample, thus optimising the amount of useful information learnt by the ANNs. The results of §3.3.2 demonstrate that, with careful selection of the training data, it is possible to apply ANNz to target samples which are somewhat fainter than the training data.

Another potential solution to this problem is to use simulated catalogues as training data. Since this requires the use

of theoretical SEDs it introduces the disadvantages of the template-based methods, such as the need for precise calibration. However, the ANN approach has advantages over standard template-matching: simulated catalogues can contain galaxies representing a large range of complex star formation histories, dust extinction models and metallicities etc., giving fully Bayesian statistics, and ANNs allow much more flexible weighting to be applied to the filters than is possible with the simple χ^2 -weighting of standard template-matching.

ACKNOWLEDGMENTS

We acknowledge help and advice from Andrew Firth, Rachel Somerville and Elizabeth Stanway. The ANN training program is based on code kindly provided by B. D. Ripley. AAC is supported by an Isle of Man Department of Education Postgraduate Studies Grant.

Comments on the ANNz package are welcomed at aac@ast.cam.ac.uk.

REFERENCES

Andreon S., Gargiulo G., Longo G., Tagliaferri R., Capuano N., 2000, MNRAS, 319, 700
 Ball N. M., Loveday J., Fukugita M., Nakamura O., Okamura S., Brinkmann J., Brunner R. J., 2003, astro-ph/0306390
 Bishop C. M., 1995, Neural Networks for Pattern Recognition. Oxford University Press
 Blum E. K., Li L. K., 1991, Neural Networks, 4 (4), 511-515
 Bolzonella M., Miralles J.-M., Pelló R., 2000, A&A, 363, 476
 Bruzual A. G., Charlot S., 1993, ApJ, 405, 538
 Coleman G. D., Wu C.-C., Weedman D. W., 1980, ApJS, 43, 393
 Connolly A. J., Csabai I., Szalay A. S., Koo D. C., Kron R. G., Munn J. A., 1995, AJ, 110, 2655
 Csabai I., Budavári T., Connolly A. J., Szalay A. S., Győry Z., Benítez N., et al., 2003, AJ, 125, 580
 Dickinson M., GOODS Legacy Team 2001, Bulletin of the American Astronomical Society, 33, 820
 Eisenstein D. J., Annis J., Gunn J. E., Szalay A. S., Connolly A. J., Nichol R. C., et al., 2001, AJ, 122, 2267
 Fernández-Soto A., Lanzetta K. M., Yahil A., 1999, ApJ, 513, 34
 Firth A. E., Lahav O., Somerville R. S., 2003, MNRAS, 339, 1195
 Jones L. K., 1990, Proceedings of the IEEE 78 (10), 1586-1589
 Lahav O., Naim A., Sodré L., Storrie-Lombardi M. C., 1996, MNRAS, 283, 207
 Le Fevre O., et al., 2003, in Discoveries and Research Prospects from 6- to 10-Meter-Class Telescopes II. Edited by Guhathakurta, Puragra. Proceedings of the SPIE, Volume 4834, pp. 173-182 (2003).
 Sowards-Emmerd D., Smith J. A., McKay T. A., Sheldon E., Tucker D. L., Castander F. J., 2000, AJ, 119, 2598
 Stoughton C., Lupton R. H., et al., 2002, AJ, 123, 485
 Strauss M. A., et al., 2002, AJ, 124, 1810
 York D. G., et al., 2000, AJ, 120, 1579